Structural transition and motion of domain walls in liquid crystals under a rotating magnetic field

Satoru Nasuno, Nobuhisa Yoshimo, and Shoichi Kai*
Department of Electrical Engineering, Kyushu Institute of Technology, Tobata, Kitakyushu 804, Japan
(Received 9 September 1994)

A sharp transition from static to propagating domain walls is observed in a homeotropic nematic layer driven by a rotating magnetic field. We show experimentally that this transition is a manifestation of the transition of wall structure from Ising type to Bloch type. We find that the initial curvature of the wall plays an important role in this transition.

PACS number(s): 61.30.Jf, 47.20.Ky, 61.30.Gd

Domain walls are common objects in both equilibrium and nonequilibrium systems where discrete symmetries are spontaneously broken. However, it has been emphasized recently that there may be crucial differences in their dynamics depending on whether the system is in equilibrium (*variational*) or in nonequilibrium (*nonvariational*) [1,2]. In the case of equilibrium systems, the motion of walls is essentially described by the evolution equations derived from a free energy and hence the wall motion is only transient until the system reaches the equilibrium state. On the other hand, in the case of nonequilibrium systems, there is no general variational principle. This fact may bring new features, such as persistent motions of walls, which are not seen in equilibrium [1–3].

The walls appearing in a nematic liquid crystal layer driven out of equilibrium by a rotating magnetic field [4] provide good examples to investigate such new features. Recent experiments [5,6] show that there is a transition from static walls to propagating walls which can form rotating spirals. Theoretical studies based on the Ginzburg-Landau-type equations [7] predict that this transition should be accompanied by the structural transition of walls, which is analogous to the Ising-Bloch transition in ferromagnetic systems [8]. However, so far there are few convincing experimental results of this structural transition. Only a little is known about the dynamics of such moving walls.

In this Brief Report we present quantitative measurements showing that the structural transition of walls indeed takes place at the transition point from static to moving walls. Our data reveal that this transition is of second order at least for weak magnetic fields, in good agreement with theoretical predictions [7]. To evaluate the curvature effect we investigate both straight and looped walls and find that the finite curvature suppresses the degeneracy of the propagating direction of walls and plays an important role in the formation of spiral patterns.

The experiments were done in a thin layer of the nematic liquid crystal, 4-methoxybenzylidene-4′-*n*-butylaniline (MBBA), confined between two parallel glass plates. The glass plates are separated by Mylar spacer to a gap of 50 μm. The horizontal dimensions of the nematic layer are 8×8 mm^2. The inner glass surfaces of the sample were coated with silane surfactant, *n,n*-dimethyl-*n*-octadecyl-3-aminopropyl-trimethoxysilyl chloride (DMOAP), to achieve homeotropic alignment, where the nematic molecules orient perpendicular to the glass plates. The temperature of the sample was regulated to $28.00 \pm 0.02\,^{\circ}$C.

Figure 1 shows a schematic diagram of our experimental setup (for more details see Ref. [9]). A static and uniform magnetic field **H** created by an electromagnet was applied parallel to the glass plates of the sample. In order to realize a rotating magnetic field against the sample, the sample was rotated at a controlled angular velocity ω about the z axis that is perpendicular to the glass surface. The angular velocities used in the present experiment are low enough that no flow occurs in a sample by rotation. The distortion of the director field is visualized by placing the sample between crossed polarizers and illuminating it from below with a white-light beam. The intensity $I(x, y)$ of a visualized image is then

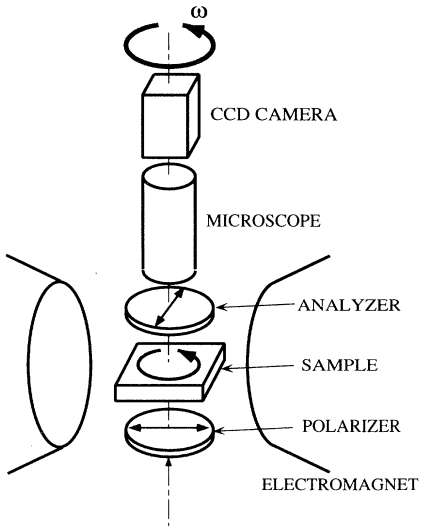

FIG. 1. Schematic diagram of the experimental setup for a rotating magnetic field. The pole piece of the electromagnet has a diameter of 80 mm.

*Present address: Department of Applied Physics, Kyushu University, Hakozaki, Higashi-ku, Fukuoka 812, Japan.

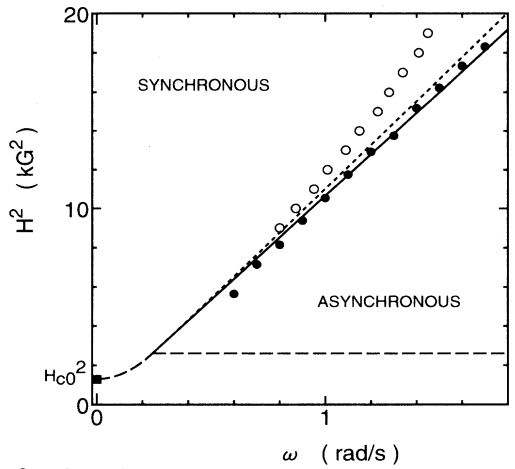

FIG. 2. Phase diagram for a thin layer of nematic liquid crystal under a rotating magnetic field. The solid square and solid circles denote the threshold for the Fréedericksz transition and the threshold for the synchronous-asynchronous transition, respectively. Open circles represent the threshold for dynamic walls. The broken and solid lines are theoretical predictions for the Fréedericksz transition and the synchronous-asynchronous transition, respectively. The dotted line is the theoretical prediction for Ising-Bloch transition.

measured with a charge-coupled-device camera, which is mounted on the microscope and rotated with the sample and analyzed with a digital image processor system ($512 \times 480 \times 8$ bits). In our sample, the critical field for the Fréedericksz transition H_{c0} was 1140 ± 10 G at $\omega = 0$.

In Fig. 2 we show the state diagram of our sample. As discussed in Refs. [4,10,7], above the threshold $H_c(\omega)$ of the Fréedericksz transition, the homeotropic state loses stability through either a pitchfork or a Hopf bifurcation and new states called synchronous or asynchronous appear. The synchronous state appears when $\omega < \omega_c = \chi_a H^2/2\gamma_1$, where χ_a is the anisotropy of the magnetic susceptibility and γ_1 the effective rotational viscosity. In this regime the molecules (director $\hat{\mathbf{n}}$) rotate about the z axis with a constant phase lag α against $\mathbf{H}$, where α is the stable-equilibrium solution of the following equation:

$$\dot{\alpha} = \omega - \omega_c \sin(2\alpha). \qquad (1)$$

This equation has two stable solutions α_0 and $\alpha_0 + \pi$ for $\omega < \omega_c$ and therefore the two different corresponding states exist [11]. The walls appear as narrow transition regions between them. In the present paper we focus on these walls.

The wall motion in a rotating magnetic field was studied by the following procedure. First walls were created at $\omega = 0$ by applying a magnetic field $H > H_{c0}$ in increments. After some time of relaxation motion of the walls, only one or a few isolated walls could be left, which were either slowly shrinking elliptical walls or stable straight walls with their ends at the lateral boundaries of the cell [12]. Then the magnetic field was set to the desired strength and rotated at a constant angular velocity ω.

First of all, the results starting from a straight-line wall will be described. The isolated straight walls are stationary when ω is below a critical value $\omega_d(H)$. When ω exceeds ω_d, the wall starts to propagate with a constant velocity v. The direction of propagation is normal to the walls in either the forward (v) or the backward ($-v$) direction, which occurs with equal possibility, indicating the degeneracy of this transition. To characterize this transition more quantitatively, we measure the propagation speed v as a function of ω for various magnitudes of magnetic field. Typical results obtained for $H^2 = 19.0$ kG^2 are shown in Fig. 3. The steep increase of v near $\omega_d \approx 1.44$ rad/s implies a transition from static to dynamic walls. The precise value of ω_d, however, is difficult to determine due to the slight rounding of the bifurcation. This rounding near ω_d may be attributable to slight imperfections such as a small deviation of the rotation axis from the z axis. We note that the experiments per-

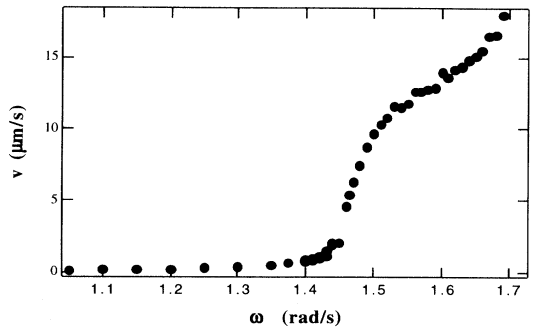

FIG. 3. Propagation speed v of isolated straight walls as a function of ω for $H^2 = 19.0$ kG^2. The synchronous-asynchronous transition occurs at $\omega = 1.73 \pm 0.03$ rad/s.

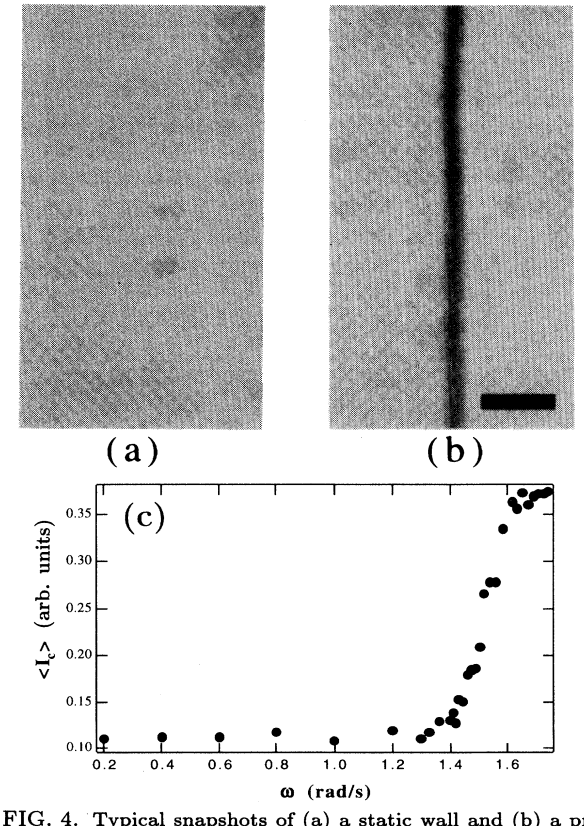

FIG. 4. Typical snapshots of (a) a static wall and (b) a propagating wall, observed under a polarized incident light (see the text). Isolated straight walls locate at the center of these pictures, although it is invisible in (a). The bar corresponds to 50 μm. (c) Average optical contrast $\langle I_c \rangle$ of walls as a function of ω for $H^2 = 19.0$ kG^2. Note that $\langle I_c \rangle$ increases steeply at the transition threshold from static to dynamic walls (see also Fig. 3).

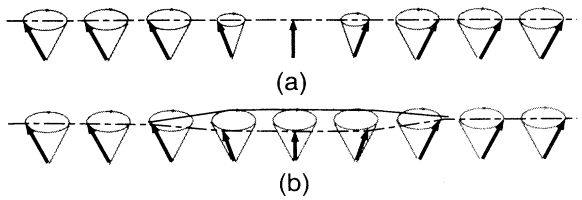

FIG. 5. Schematic illustration of two possible structures of walls: (a) static (Ising) wall and (b) propagating (Bloch) wall. The directors (indicated by arrows) rotate synchronously on the surfaces of the cones following the magnetic field. In the Ising wall the director points along the z axis at the center, while it does not in the Bloch wall. Note that two symmetric structures of opposite chirality (indicated by solid and dotted lines) are possible in the case of the Bloch wall.

formed by both continuously increasing and decreasing ω yield the same results as Fig. 3 and there was no measurable hysteresis within our experimental resolution. It is in clear contrast to previous experiments performed for higher field strengths [5] and in good qualitative agreement with recent theoretical predictions assuming weak field strengths [7].

A significant distinction between the stationary walls and the propagating walls can be made optically if the analyzer is removed and if the polarizer is set so that the incident light beam is polarized normal to the plane Σ spanned by the z axis and the director $\hat{\mathbf{n}}$ in the homogeneous domains, as mentioned in Ref. [5]. Under such an optical configuration, the static wall becomes difficult to observe optically [Fig. 4(a)], although the dynamic wall is still visible as a dark line [Fig. 4(b)]. To characterize this optical difference quantitatively, we measured the optical contrast I_c of the straight walls as a function of ω for several values of H. The contrast I_c was defined by the difference between the maximum and the minimum intensity of the optical profile measured along a line across the wall. We found that the contrast I_c was not constant in time, but slightly oscillated around a mean value during one period T of the field rotation. Hence we computed the mean contrast $\langle I_c \rangle$, averaged over one period. The typical results obtained for $H^2 = 19.0$ kG^2 are shown in Fig. 4(c). The increase of $\langle I_c \rangle$ near $\omega \approx 1.4$ rad/s is quite drastic. This sharp change in $\langle I_c \rangle$ coincides

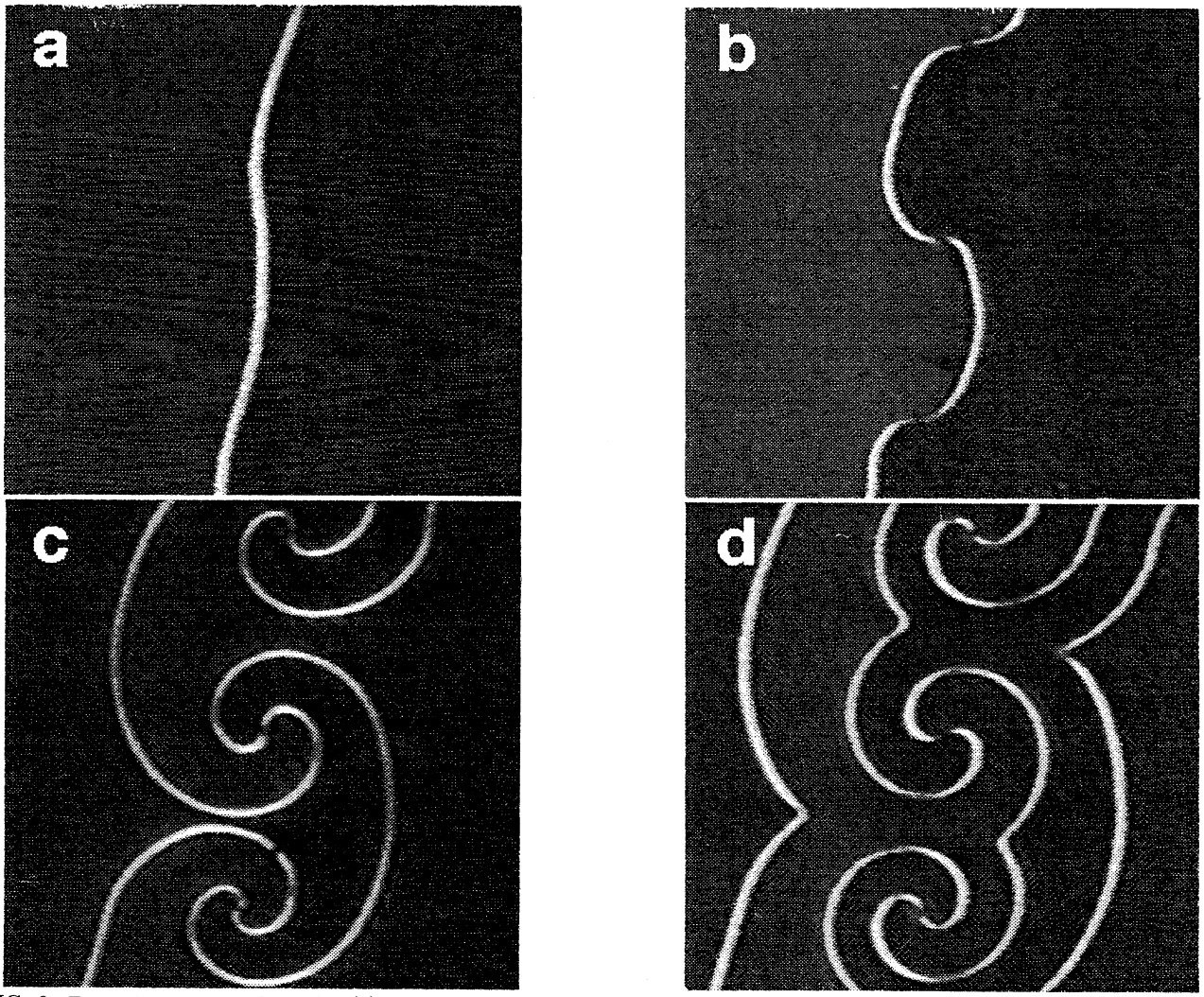

FIG. 6. Formation process of spirals. (a) At $t = 0$ the angular frequency ω is increased suddenly from zero to 1.37 rad/s keeping $H^2 = 16.0$ kG^2. (b), (c), and (d) correspond to $t = 23$, 53, and 65 s, respectively. The magnetic field is rotating clockwise. The patterns are observed under crossed polarizers.

with the transition from stationary to propagating walls (see Fig. 3).

According to the optical properties of nematic liquid crystals [13], the change in $\langle I_c \rangle$ implies the transition of the director configuration within the walls: In the static wall the director should be parallel to the Σ plane everywhere to make the wall invisible. On the other hand, in the propagating wall the director should make a finite angle with respect to the Σ plane to make the wall visible. Figure 5 shows the possible structures of such walls. Across the static wall shown in Fig. 5(a), the director points along the z axis at the center and the phase lag α suffers a jump of π there, while across the propagating wall shown in Fig. 5(b) α changes smoothly by $\pm\pi$. These structures are the theoretically predicted ones [1,7]; the former structure is referred to as the Ising wall and the latter as the Bloch wall, in analogy with ferromagnetic systems. As shown in Fig. 5(b), two different rotations of the director are possible in the Bloch wall. These two possibilities for the wall structure lead the degeneracy of the propagating direction, as discussed in Refs. [1,6,7]. More precisely speaking, the propagating direction of the Bloch wall is determined by their chirality defined with respect to the rotational direction of the magnetic field [9]. As a result, if the rotation of the magnetic field is reversed suddenly, then the wall starts to propagate in the opposite direction with the same speed.

In a first approximation, the transmitted light intensity is proportional to the square of the spatial variation of the effective reflection index for the incident light. Then the contrast I_c of propagating walls should increase as the tilt angle of the director with the z axis at the center of the wall increases and as the wall width decreases. The width of the wall remains almost of the same order for ω near ω_d. Therefore, $\langle I_c \rangle$ provides a measure for the amount of deviation of the director from the z axis at the center of the walls at least near ω_d. On these grounds our result shown in Figs. 3 and 4 indicates that the propagation speed increases as the director deviates from the z axis at the center of walls.

Second, in order to evaluate the curvature effect, we investigated also the dynamics of looped walls with various diameters. The experiments were done mainly at $H^2 = 19.0$ kG^2 by preparing an isolated looped wall at $\omega = 0$ and then jumping ω in a steplike manner above ω_d. When we started from the looped wall with sufficiently large diameters, the looped wall propagated either outward or inward with almost equal possibility in different runs. However, when we started with small diameters, only outward motion was observed. The above observations indicate that the curvature suppresses the degeneracy of the wall structure and the walls tend to start propagating in the convex direction rather than the concave direction. For a sufficiently large diameter limit, the curvature effect is negligible and one recovers the degeneracy of forward and backward propagation. We found also that the curvature effect played an important role in the dynamics of walls [9]. When a loop expands, for example, the wall propagates outward, always in the form of symmetric circle. On the other hand, when a loop shrinks, the wall often has nonperiodic distortion.

It sometimes happened that one static wall was simultaneously transformed into segments of counterpropagating walls upon increasing ω beyond ω_d. In such a case the walls started to rotate around the singular points connecting them and evolved into steadily rotating spirals (Fig. 6). As is obvious from this formation process, the resulting spirals always had two arms. Spiral pattern formation was more frequently observed when we started from the walls initially wavy rather than straight. In such a case the singular points appeared at the inflection points of the wall and the spiral wall pattern formed by propagation in each local convex direction (see Fig. 6). This is consistent with the results of the curvature effect mentioned above.

The transition of the wall structure from Ising to Bloch type has been observed also under a nonrotating magnetic field if an electric field is simultaneously applied across the nematic layer [14,7]. In this case, however, the system is completely variational, i.e., one can define a free energy of the system, and the straight Bloch-type walls remain stationary, in clear contrast to the present experiments.

In conclusion, we have shown experimentally that the transition from static to propagating walls in a homeotropic nematic layer under a rotating magnetic field is a manifestation of the Ising-Bloch structural transition of walls. We have further shown that the local curvature of walls breaks the degeneracy of this transition and plays an important role in the formation of spirals.

The authors would like to thank T. Yamaura and T. Yoshikawa for experimental assistance. We also acknowledge T. Mizuguchi and F. Sagués for valuable discussions and comments. This work is partially supported by Grant-in-Aids for Scientific Research from the Ministry of Education, Science, and Culture of Japan (Grant No. 04854022).

[1] P. Coullet *et al.*, Phys. Rev. Lett. **65**, 1352 (1990).
[2] A. Hagberg and E. Meron, Phys. Rev. E **48**, 705 (1993).
[3] H. Ikeda *et al.*, Nonlinear Anal. **13**, 507 (1989).
[4] F. Brochard *et al.*, J. Phys. (Paris) Colloq. **36**, C1-209 (1975).
[5] K.B. Migler and R.B. Meyer, Phys. Rev. Lett. **66**, 1485 (1991); Phys. Rev. E **48**, 1218 (1993).
[6] K.B. Migler and R.B. Meyer, Physica D **71**, 412 (1994).
[7] T. Frish *et al.*, Phys. Rev. Lett. **72**, 1471 (1994).
[8] J. Lajzerowicz and J.J. Niez, J. Phys. (Paris) Lett. **40**, L-165 (1979).
[9] S. Nasuno *et al.* (unpublished).
[10] F. Sagués, Phys. Rev. A **38**, 5360 (1988).
[11] These two stable states disappear through a saddle-node bifurcation at ω_c.
[12] L. Leger, Solid State Commun. **11**, 1499 (1972).
[13] L.M. Blinov, *Electro-optical and Magneto-optical Properties of Liquid Crystals* (Wiley, Chichester, 1983).
[14] J.M. Gilli *et al.*, J. Phys. (France) II **4**, 319 (1994).

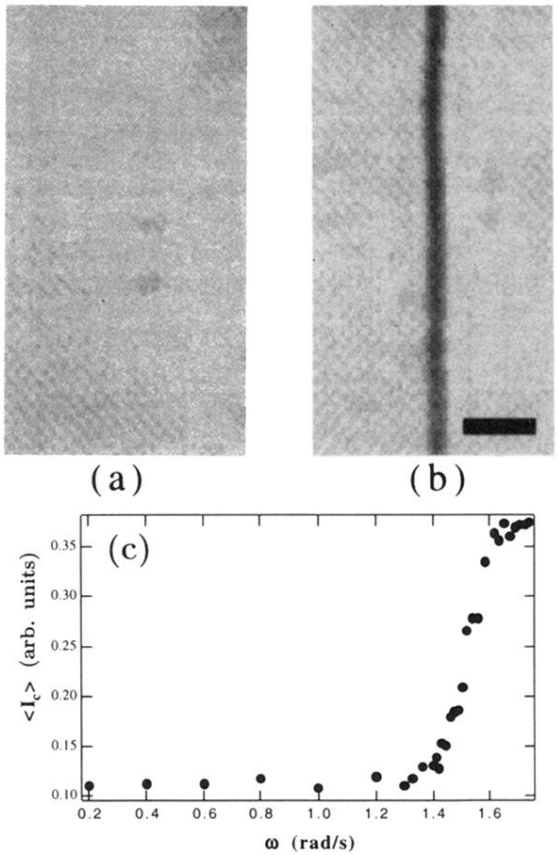

FIG. 4. Typical snapshots of (a) a static wall and (b) a propagating wall, observed under a polarized incident light (see the text). Isolated straight walls locate at the center of these pictures, although it is invisible in (a). The bar corresponds to 50 μm. (c) Average optical contrast $\langle I_c \rangle$ of walls as a function of ω for $H^2 = 19.0$ kG^2. Note that $\langle I_c \rangle$ increases steeply at the transition threshold from static to dynamic walls (see also Fig. 3).

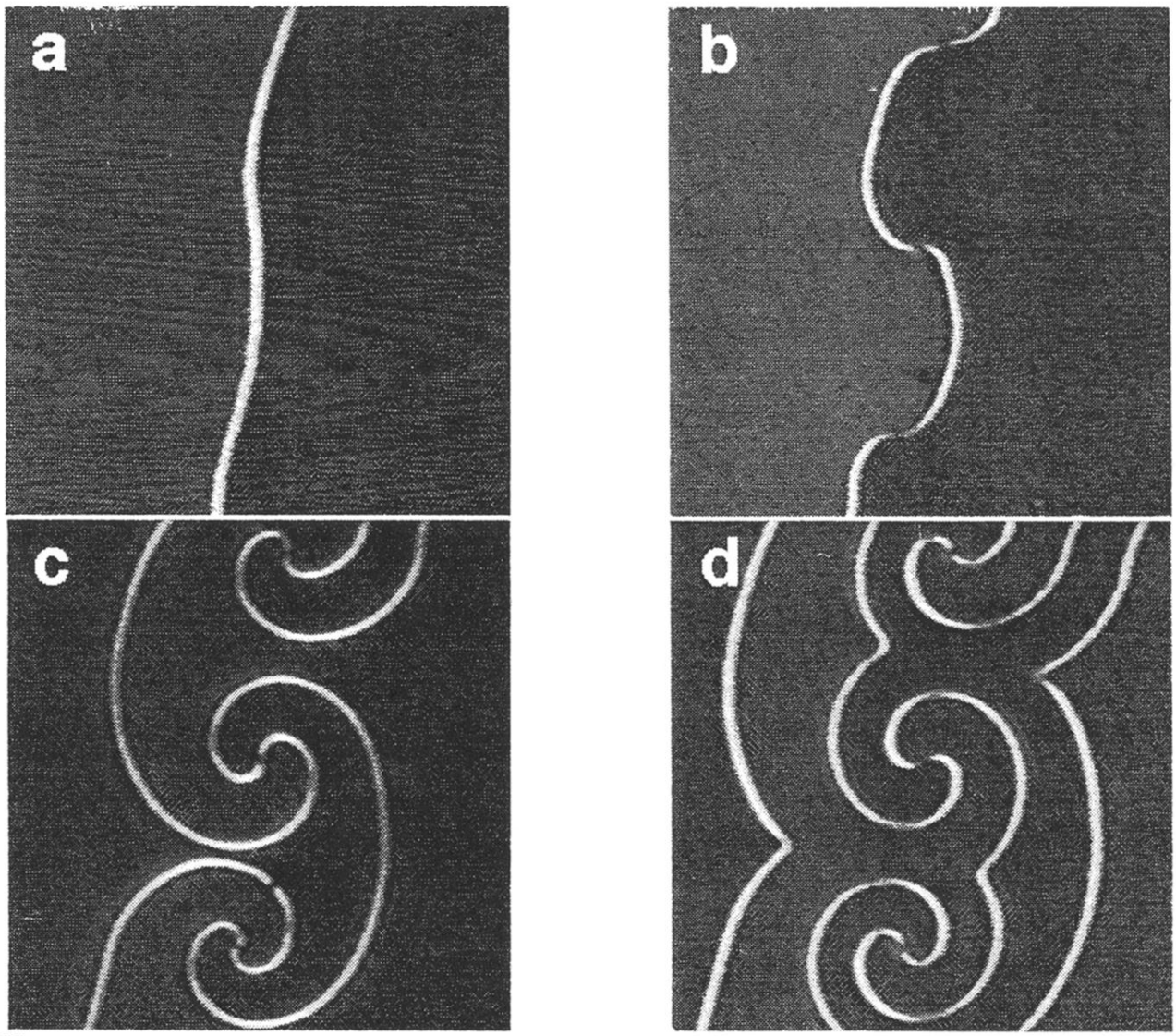

FIG. 6. Formation process of spirals. (a) At $t = 0$ the angular frequency ω is increased suddenly from zero to 1.37 rad/s keeping $H^2 = 16.0$ kG^2. (b), (c), and (d) correspond to $t = 23$, 53, and 65 s, respectively. The magnetic field is rotating clockwise. The patterns are observed under crossed polarizers.